

Solar oscillations: time analysis of the GOLF p -mode signal

C. Renaud¹, G. Grec¹, P. Boumier², A.H. Gabriel², J.M. Robillot³, T. Roca Cortés⁴, S. Turck-Chièze⁵, and R.K. Ulrich⁶

¹ Département Cassini, UMR 6529 du CNRS, Observatoire de la Côte d’Azur, F-06304 Nice, France

² Institut d’Astrophysique Spatiale, Unité Mixte CNRS et Université Paris XI, F-91405 Orsay, France

³ Observatoire de l’Université Bordeaux 1, B.P. 89, F-33270 Floirac, France

⁴ Instituto de Astrofísica de Canarias, E-38205 La Laguna, Tenerife, Spain

⁵ Service d’Astrophysique, DSM/DAPNIA, CE Saclay, F-91191 Gif-sur-Yvette, France

⁶ Astronomy Department, University of California, Los Angeles, USA

Received 30 October 1998 / Accepted 12 March 1999

Abstract. We determine the intrinsic phase lag of the GOLF data for the solar p -mode velocity deduced either from one of the narrow band photometers working alternatively on blue and red wing of the sodium lines. The timing of the “blue wing” velocity coming from the current GOLF data is given in respect to the ground-based observations. The phase lag for the “blue” velocity is 6 s in advance relatively to a velocity coming from a differential device. For individual p modes, the phase lag from the “blue” velocity to the “red” velocity are not in opposition of phase, as expected in a very simple solar model, but differs from 8° to 18° from the opposition, depending on the degree and the radial order of the acoustic mode. The measurement of the differential lag between the blue and red wings of the D lines may open a new way to monitor the temperature oscillations with the optical depth.

Key words: Sun: oscillations

1. Introduction

As the other instruments devoted to the measurement of the velocity averaged over the disk of the sun observed as a star, GOLF (Gabriel et al., 1995) is a differential device. The technical principle is to measure the Doppler wavelength shift of the D Fraunhofer lines of sodium produced in the solar atmosphere. The photometric signal contains successive samples of the intensity in the blue or red wing of the line profiles of DI and DII. Moreover, due to the failure of the mechanical control of the optical band pass, the present measurements are made only on the blue wing from which we deduce a “blue” velocity signal. This new observational figure rises the problem of the phase comparison with the observations made with the ground-based instruments. Previous works reveal a phase lag from GOLF to MKI (Régulo et al., 1996, Pallé et al., 1999) and MDI (Henyey et al., 1998). Moreover, those results are all dependent on the exact timing of several sequences of data, as the uncertainties increase with the number of steps involved in the timing

process. We calculate there the phase lag for the crude GOLF measurements for the p -mode frequencies, using only the internal clock of the instrument. The first part of the paper shows that the blue and red wings of the sodium lines are not in opposition of phase. Due to this phase lag, the “blue” velocity is 6 s in advance relatively to a velocity coming from a differential device.

The second part is devoted to the analysis of the “blue” to the “red” phase lag, for individual p modes. When the very simple solar model predicts an opposition of phase, the observed phases differ from 8° to 18° from this opposition, depending on the degree and the radial order of the acoustic mode.

A simulation using real solar data gives the uncertainties related to the numerical method and shows the statistical significance of all results.

2. The GOLF measurement sequence

The GOLF instrument measurements are driven by a precise on-board clock, the timing is made at the beginning of the 80 s software cycle with the reading of the LOBT τ_0 (local on board time¹). We use the same timing for the present time analysis. Nevertheless, as the blue and red channel measurements are made in sequence, an instrumental delay is directly related to the integration time:

For the first period, from Jan. 18 to Feb. 10, 1996, the sequence was “blue wing” signal for 10 s, “red wing” signal for 10 s and so on. When the values of both signals are averaged over the 80 s cycle, the mean measurement time related to this process is $T_{b1} = \text{TAI} + 34.5$ s for the “blue” signal and $T_{r1} = \text{TAI} + 44.5$ s for the “red” signal. This period was devoted to instrumental tests, we use only the data from Jan. 26 to Feb. 6.

For the second period, from Feb. 18 to Mar. 31, 1996, the sequence was “red” signal for 10 s, “blue” signal for 10 s and

¹ The SOHO timing is given in TAI (Temps Atomique International), from which UTC (Coordinated Universal Time, related to the Earth’s rotation) differs by an integer number of seconds. For 1996 and 1997, up to Jun. 30 at 24h, $\text{UTC} = \text{TAI} + 30$ s. For the rest of 1997 and 1998 $\text{UTC} = \text{TAI} + 31$ s. An additional second will come in 1999, Jan. 1st.

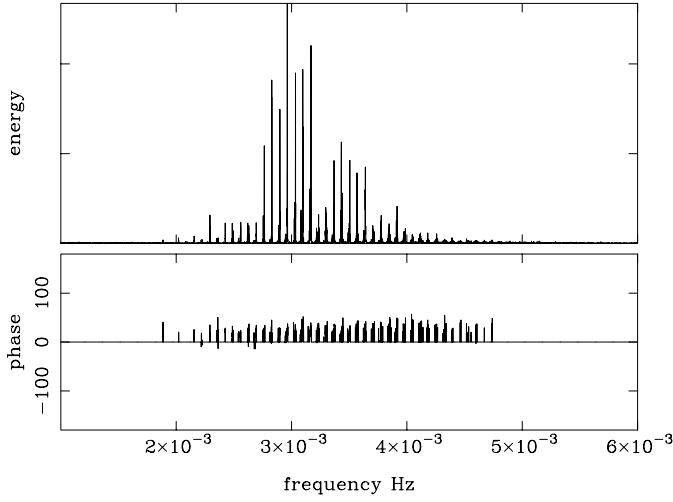


Fig. 1. Amplitude and phase of the cross-spectrum of the opposite of the red signal and the blue signal from Jan 26 to Feb 6, 1996.

so on. On the same 80 s integration interval, the mean measurement time is $T_{b2} = \text{TAI}+44.5$ s for the “blue” signal and $T_{r2} = \text{TAI}+34.5$ s for the “red” signal.

For the third period, from Apr. 10, 1996, to Jun. 24, 1998, the measurements are on the blue wing only, $T_{b3} = \text{TAI}+39.5$ s.

For all periods, each of the 10 s measurement is splitted in 2 parts, the optical band-pass being slightly shifted every 5 s.

SOHO receives the solar light 5 s earlier than a ground-based observatory. The on board generated timing is not corrected for this delay.

3. The temporal cross-correlation for the photometric signal

We measure here the delay of the “red” velocity in respect to the “blue” velocity. From the GOLF photometric signals $I_r(t)$ and $I_b(t)$ (i.e. the number of photons counted during a 10 s time interval), we define the velocity $F_r(t)$ and $F_b(t)$ as their relative variations, using as photometric reference the slowly varying functions $I_r^*(t)$ and $I_b^*(t)$ (Eqs. 1 & 2). $I_r^*(t) = \mathcal{F} I_r(t)$ and $I_b^*(t) = \mathcal{F} I_b(t)$, where \mathcal{F} is a numerical filter selecting the temporal harmonics of period longer than 12 h.

This first level of calibration rejects the instrumental changes of the sensitivity relating the photometric signal to the Doppler shift (a simple example of this change of the sensitivity is the light modulation due to the varying solar distance). We use a FFT algorithm to compute the Fourier transforms $\tilde{F}_r(\nu)$ and $\tilde{F}_b(\nu)$ and then compute the cross-spectrum $\mathcal{C}(\nu)$ (Eq. 3).

$$F_r(t) = I_r(t) / I_r^*(t) \quad (1)$$

$$F_b(t) = I_b(t) / I_b^*(t) \quad (2)$$

$$\mathcal{C}(\nu) = \tilde{F}_r(\nu) \cdot \overline{\tilde{F}_b(\nu)} \quad (3)$$

$\overline{\tilde{F}(\nu)}$ is the complex conjugate of $\tilde{F}(\nu)$.

From this analysis and if there is no intrinsic phase lag in the solar signals, we should obtain the time lag relative to the measurement sequence sketched in the Sect. 2.

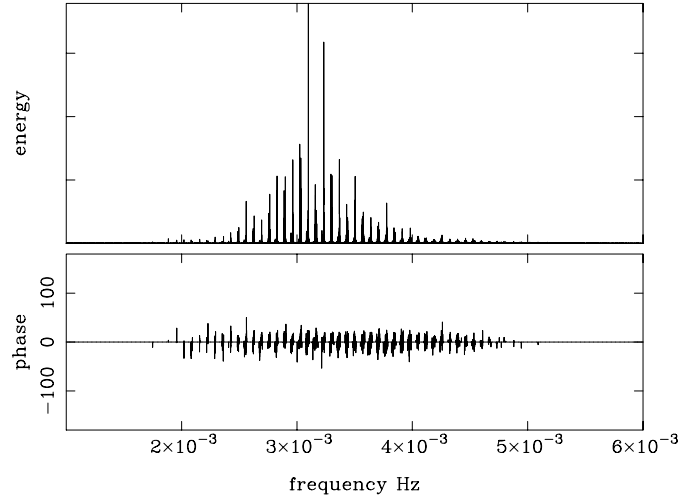


Fig. 2. Amplitude and phase of the cross-spectrum of the opposite of the red signal and the blue signal from Feb 18 to Mar 31, 1996. The visible difference in phase with Fig. 1 results from a different setting of the hardware.

The Fig. 1 and Fig. 2 show the amplitude and phase of the cross-spectrum $\mathcal{C}(\nu)$ obtained for the 2 periods of differential observation.

The cross-spectrum is sampled on the discrete frequencies ν_j , the amplitude $\mathcal{A}(\nu_j)$ and phase $\phi(\nu_j)$ are defined as $\mathcal{C}(\nu_j) = \mathcal{A}(\nu_j) \exp 2i\pi\phi(\nu_j)$. Then, for a given set of p modes, we calculate the average of the phase for the bins where $\mathcal{A}(\nu_j) \geq \mathcal{A}_{th}$. The threshold \mathcal{A}_{th} is adjusted to restrict the integration to the energy values above the noise level in the power spectrum.

The phase $\phi_{n,l}$ is computed on narrow band surrounding the modes of degrees $l = 0, 2$ or $l = 1, 3$ respectively, using a p -mode frequency table (Lazrek et al., 1997). For each bin, the angular lag is weighted proportionally to the amplitude (Eq. 4). In the same way, the averaged delay $\delta_{n,l}$ is deduced from the angular lag $\phi(\nu_j)$ and from the frequency ν_j for each bin (Eq. 5).

$$\phi_{n,l} = \frac{\sum_j \phi(\nu_j) \cdot \mathcal{A}(\nu_j)}{\sum_j \mathcal{A}(\nu_j)} \quad (4)$$

$$\delta_{n,l} = \frac{\sum_j \phi(\nu_j) / \nu_j / 2\pi \cdot \mathcal{A}(\nu_j)}{\sum_j \mathcal{A}(\nu_j)} \quad (5)$$

The Tables 1 and 2 show the results for the mean phase and the energy in arbitrary scale for the highly excited p -modes. The mean delay is $\delta \simeq 22$ s for the period 1 and $\delta \simeq 2$ s for the period 2. We found here the offset of 20 s predicted from the change in the procedure. This offset is relative to the instrument, but allows a non-ambiguous verification of the sign of the relative phase of the 2 channels. Taking into account the hardware generated delay of 10 s, the opposite of the red signal is late in respect to the blue, with a mean delay $\delta \simeq 12$ s. The Fig. 3 shows the delay $\delta_{n,l}$ for the observable range of the order n of the p mode, for the 2 periods of differential observations (cf. Sect. 2). In Sect. 7 we shall go farther in the details of the measurement of the p -mode phases, let first discuss the present result.

Table 1. The values of the cross-spectrum phase $\Phi_{n,l}$ and the related delay $\delta_{n,l}$ for the p modes observed in the period from Jan 26 to Feb 6, 1996, for the opposite of the signal in the red wing and the signal in the blue wing.

n,l	energy	phase $\Phi_{n,l}$ (d°)	delay $\delta_{n,l}$ (s)
16, 1 & 15, 3	0.10	22.19	25.50
17, 1 & 16, 3	0.15	20.07	21.86
18, 1 & 17, 3	0.12	22.96	23.75
19, 1 & 18, 3	0.66	23.25	22.90
20, 1 & 19, 3	0.99	24.34	22.88
21, 1 & 20, 3	1.00	25.44	22.87
22, 1 & 21, 3	0.35	23.71	20.42
23, 1 & 22, 3	0.63	25.87	21.39
24, 1 & 23, 3	0.52	25.08	19.92
25, 1 & 24, 3	0.59	28.41	21.72
26, 1 & 25, 3	0.27	28.88	21.29
27, 1 & 26, 3	0.30	29.92	21.28
28, 1 & 27, 3	0.12	33.08	22.74
17, 0 & 16, 2	0.13	18.49	20.63
18, 0 & 17, 2	0.20	19.75	20.91
19, 0 & 18, 2	0.51	24.79	24.97
20, 0 & 19, 2	0.52	22.90	21.99
21, 0 & 20, 2	0.84	25.83	23.70
22, 0 & 21, 2	0.95	25.88	22.73
23, 0 & 22, 2	0.50	26.09	21.98
24, 0 & 23, 2	0.77	24.31	19.67
25, 0 & 24, 2	0.49	25.28	19.68
26, 0 & 25, 2	0.28	29.40	22.05
27, 0 & 26, 2	0.28	31.16	22.54
28, 0 & 27, 2	0.18	31.53	22.02
29, 0 & 28, 2	0.17	29.26	19.76
mean value			22.10

4. The GOLF p -mode signal

The photometric signal related to the velocity measurement contains 2 components:

- The p -mode velocity oscillations produce a line drift in respect to the local reference, the slope of the wing of the observed line governing the change in the monochromatic intensity. Thoses changes are opposite in phase for the “blue” and “red” channel, and roughly of same amplitude.
- The p modes produce a change in the temperature of the photosphere, observed in wide band photometry, firstly observed with the ACRIM instrument on board the SMM satellite (Woodard & Hudson, 1983). Even as an hypothesis, we can assume that the same temperature effect is present in the sodium lines.

If we scale the AC signal relatively to the DC photometric component, the integrated p -mode amplitude $A \simeq 1.5 \text{ m s}^{-1}$, gives in the GOLF blue and red channel a signal $I_V \simeq 3.6 \cdot 10^{-4}$; the p -mode wide-band photometry signal $I_T \simeq 10^{-5}$ and finally $r_p = I_T / I_V \simeq 0.028$ for both channels. The wide-band signal gives an additional photometric component, due to the diffuse

Table 2. The values of the cross-spectrum phase $\Phi_{n,l}$ and the related delay $\delta_{n,l}$ for the p modes observed in the period from Feb 18 to Mar 31, 1996, for the opposite of the signal in the red wing and the signal in the blue wing.

n,l	energy	phase $\Phi_{n,l}$ (d°)	delay $\delta_{n,l}$ (s)
17, 1 & 16, 3	0.12	2.66	2.90
18, 1 & 17, 3	0.11	1.97	2.04
19, 1 & 18, 3	0.32	2.24	2.20
20, 1 & 19, 3	0.55	2.39	2.25
21, 1 & 20, 3	1.00	3.05	2.74
22, 1 & 21, 3	0.87	1.75	1.51
23, 1 & 22, 3	0.52	3.52	2.91
24, 1 & 23, 3	0.43	2.07	1.65
25, 1 & 24, 3	0.25	2.34	1.79
26, 1 & 25, 3	0.27	3.14	2.32
27, 1 & 26, 3	0.14	3.92	2.78
17, 0 & 16, 2	0.10	3.07	3.43
18, 0 & 17, 2	0.18	1.96	2.07
19, 0 & 18, 2	0.36	2.83	2.85
20, 0 & 19, 2	0.43	3.49	3.35
21, 0 & 20, 2	0.96	0.80	0.74
22, 0 & 21, 2	0.64	0.59	0.52
23, 0 & 22, 2	0.70	3.22	2.71
24, 0 & 23, 2	0.38	1.16	0.94
25, 0 & 24, 2	0.50	2.22	1.72
26, 0 & 25, 2	0.28	−0.38	−0.29
27, 0 & 26, 2	0.21	1.68	1.22
28, 0 & 27, 2	0.13	0.02	0.01
mean value			1.97

light in the device. The relative sensitivity is $\simeq 0.03$ for the DC components, so the AC component is negligible.

The resulting signal comes out of a simple analysis of the periodic case: for the blue channel let I_{V_b} be the velocity component, I_T the intensity changes, S_b the real signal, resulting from a simple addition (cf. Eqs. 7 & 8). The Eq. 9 gives the result of the computation of the phase Φ_b of the composite signal vs. the phase φ and the amplitude ratio r defined for I_T in the Eq. 6.

$$\begin{aligned} I_{V_b} &= \cos(\omega t) \\ I_T &= r \cos(\omega t + \varphi) \end{aligned} \quad (6)$$

$$S_b = I_{V_b} + I_T \quad (7)$$

$$= A \cos(\omega t + \Phi_b) \quad (8)$$

$$\Phi_b = \arctan\left(\frac{r \sin \varphi}{1 + r \cos \varphi}\right) \quad (9)$$

Fig. 4 gives the variations of Φ_b vs. φ and r .

For the red channel, we have

$$I_{V_r} = \cos(\omega t + \pi)$$

$$\begin{aligned} S_r &= -(I_{V_r} + I_T) \\ &= A \cos(\omega t + \Phi_r) \end{aligned}$$

the phase of the signal S_r is $\Phi_r \simeq -\Phi_b$, and we get from the observations $\Phi_g = \Phi_b - \Phi_r$.

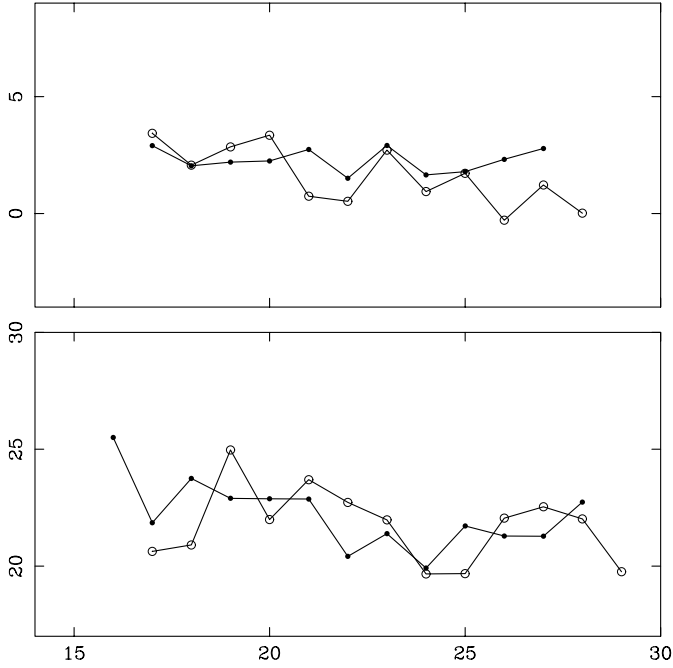


Fig. 3. The delays $\delta_{n,l}$ for close pairs of modes vs. the order n for the lower of 2 degree $l=0,2$, (\circ) and $l=1,3$ (\bullet). The lower panel corresponds to the first period of observation, the upper panel corresponds to the second period of observation. The vertical scale is the delay in s. The horizontal scale is the radial order n .

We can deduce there the delay from the blue to the red signal as $\Delta \simeq F_p \times (\Phi_r - \Phi_b) / 2\pi$, where $F_p \simeq 300$ s.

The delay $\delta = 12$ s obtained in Sect. 3 gives the value $\Phi_b \simeq 7.2^\circ$, giving the minimum value for the intensity component $r = 0.12$ if velocity and intensity phase difference is close to $\varphi = \pi/2$.

The relative phase of velocity and luminosity variations related to the p -mode oscillations is found in the literature, 90° in the adiabatic case (Jiménez et al., 1988), $119 \pm 3^\circ$ with an improved physical model of the solar atmosphere (Schrijver et al., 1991). A minimum of intensity is followed by a maximum of red-shift, ie. a minimum in the red channel intensity. The result is a negative phase shift in the red channel, as we observe in Sect. 3. The minimum value of r corresponds to the adiabatic prediction, a value close to 120° as predicted in the non-adiabatic case increasing slightly the result for r (cf Fig. 4).

This result $r = 0.12$ is 4 to 5 times higher than the predicted value $r_p = I_T / I_V \simeq 0.028$ given in the first part of the section. Moreover, our estimate of r_p is very crude. GOLF works on the sodium lines, and the depth of formation of the D lines go down to the temperature minimum. The GOLF band-pass are roughly mid-way between this minimum and the photosphere. The intensity measurements as ACRIM and VIRGO (Fröhlich et al., 1995) are made at the photospheric level. The amplitude oscillations are higher going to the chromosphere, and we may just have a measurement of this increasing amplitude, resulting in an increase of r_p .

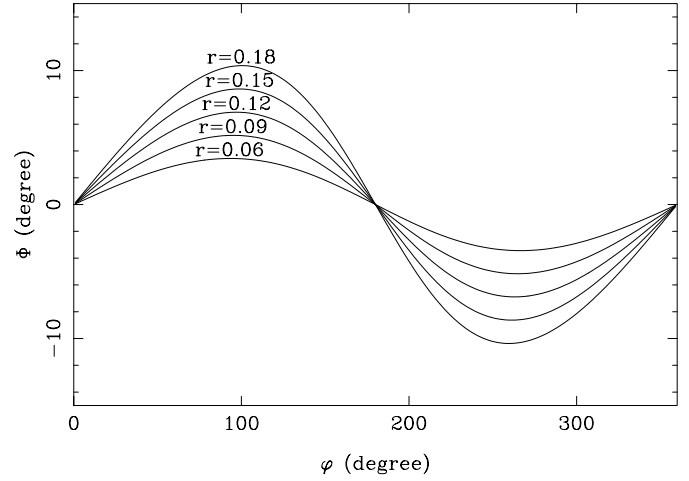


Fig. 4. The result of a crude analytic study of the phase Φ_b of the blue signal, vs. the relative amplitude r and the relative phase φ of the temperature-driven photometric component with respect to the signal due to the Doppler shift.

5. Numerical uncertainties

The GOLF data are limited to the period 2 for the more valuable “blue” vs. “red” phase study. The period 1 is shorter but gives comparable results. For the following period, from Apr. 10, 1996, to Jun. 24, 1998, the solar signal measurements are on the blue wing only. Those data are used for a simulation of the phase study made in Sect. 3, the simulated “blue” channel being the values of $F_b(t)$ (cf. Eq. 2) for odd rank time intervals, the simulated “red” channel being the values of $F_b(t)$ for even rank time intervals. The duration of each time interval is 10 s and the 2 channels have a lag $t_l = 10$ s. We can there exclude any lag coming from solar origin, but the data are valuable for a realistic test of the numerical method. We use this 805 days long period to reproduce 18 times a 44 days experiment comparable to the period 2. Thanks to the instrumental sampling, the photon noise is not correlated for the 2 channels. Fig. 5 shows the delay $\delta_{n,l} \simeq t_l$ and the standard deviation σ ; $|\delta_{n,l} - t_l| < \sigma$ in all cases excepted one low-energy mode. The standard deviation for the 18 experiments is $\sigma \simeq 1$ s or less for the high-energy modes, this value is comparable to the variation of the delay found in the Sect. 3 for the “blue” and “red” velocities.

6. “Differential” velocity vs. “GOLF” velocity

The “Differential” velocity is at first order

$$V_d = V_0 (S_b - S_r) / (S_b + S_r).$$

The ratio I_{V_b} / I_{V_r} and the sensitivity V_0 (related to the local slope of the wing) are subject to seasonal changes (plus daily changes for the ground based experiments). Moreover, the first order result will be $\Phi_d = 0.5 (\Phi_r - \Phi_b)$, and finally the differential velocity should be 6 s latter than the “blue” velocity. To check this, we applied the technique described in Sect. 3 to these 2 signals; the results are shown in the Table 3. The mean time of measurements was $T_{b2} = \text{TAI} + 44.5$ s for the “blue” signal, T_{r2}

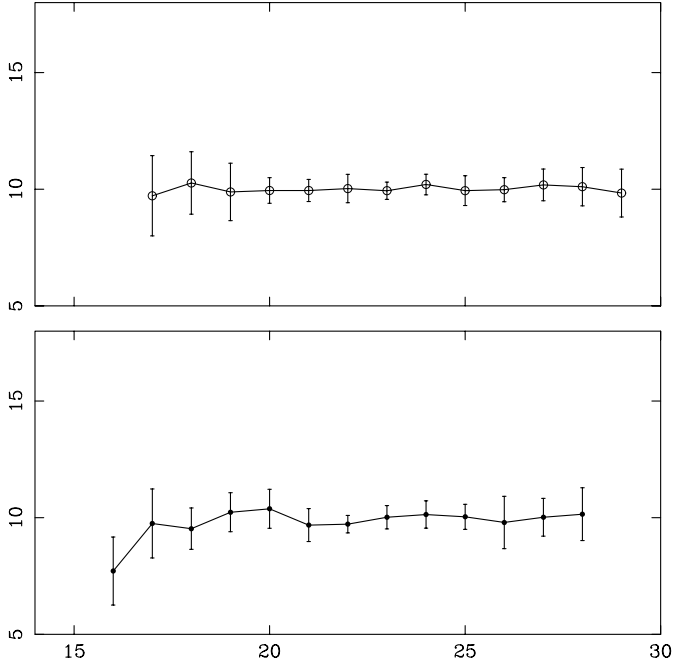


Fig. 5. Uncertainty of the numerical method. We analyse 18 simulations of the period 2, using the blue data observed for the period 3. In this case, no lag comes from the solar signal itself, a 10 s. lag is generated in the data processing. The upper panel corresponds to the modes of degree $l=0,2$ (\circ), the lower panel corresponds to the modes of degree $l=1,3$ (\bullet). The vertical scale is the delay in s. The horizontal scale is the radial order n .

= TAI+34.5 s for the “red” signal, resulting in $T_{d2} = \text{TAI}+39.5$ s for the “differential” signal. We have then to take into account a delay of 5 s due to the data acquisition. The Table 3 shows the delay $\delta_{n,l}$. The mean value is $\delta_2 \simeq 1$ s and then the true solar delay is $\delta_S \simeq 6$ s. The numerical simulation (cf. Sect. 5) allows to conclude to the solar origin of this delay, with a value $\delta_S \simeq 6 \pm 1$ s.

The status of GOLF has been changed on April 10, 1996 in a probably definitive way. All measurements are on the blue side, resulting in a mean time TAI+39.5 s for the “blue” velocity. As the “blue” GOLF velocity is 6 s earlier than the differential, the right timing for the p -mode phase measurement with another differential instrument is $T_{b3} = \text{TAI}+33.5$ s². A phase lag has no impact on the comparison of independently computed power spectra, but the timing must be considered carefully in long term merging of data coming from GOLF and from a differential instrument. The frequency of a p mode is $\simeq 3$ mHz and for the non-radial modes the rotational splitting is $\simeq 1$ μ Hz. Then the periods of 2 successive modes in a multiplet l and n differ from $\simeq 0.11$ s and a 6 s delay corresponds to the relative phase shift of one mode to the other after $\simeq 5$ h. If the timing correction is not made, 2 splitted solar modes will melt in the power spectrum as an unpredictable broad peak depending on the duty cycles

² Recall that GOLF is $\simeq 5$ s closer to the sun than the earth and TAI - UT is subject to change. The present result doesn’t take into account those additional lags.

Table 3. The values of the cross-spectrum phase $\Phi_{n,l}$ and the related delay $\delta_{n,l}$ for the p modes observed in the period from Feb 18 to Mar 31, 1996, for the differential velocity signal and the signal in the blue wing.

n,l	energy	phase $\Phi_{n,l}$ (d $^\circ$)	delay $\delta_{n,l}$ (s)
17, 1 & 16, 3	0.12	1.51	1.64
18, 1 & 17, 3	0.11	1.20	1.24
19, 1 & 18, 3	0.32	1.28	1.26
20, 1 & 19, 3	0.54	1.33	1.25
21, 1 & 20, 3	1.00	1.80	1.62
22, 1 & 21, 3	0.88	0.98	0.84
23, 1 & 22, 3	0.54	2.16	1.78
24, 1 & 23, 3	0.46	1.13	0.90
25, 1 & 24, 3	0.26	1.41	1.07
26, 1 & 25, 3	0.29	1.76	1.30
27, 1 & 26, 3	0.15	2.27	1.61
17, 0 & 16, 2	0.10	1.97	2.20
18, 0 & 17, 2	0.17	1.11	1.17
19, 0 & 18, 2	0.35	1.56	1.58
20, 0 & 19, 2	0.44	2.06	1.98
21, 0 & 20, 2	0.96	0.48	0.44
22, 0 & 21, 2	0.61	0.66	0.58
23, 0 & 22, 2	0.73	1.72	1.45
24, 0 & 23, 2	0.39	0.72	0.58
25, 0 & 24, 2	0.51	1.12	0.87
26, 0 & 25, 2	0.29	-0.17	-0.13
27, 0 & 26, 2	0.23	1.14	0.82
28, 0 & 27, 2	0.14	0.12	0.08
mean value			1.15

of the instruments. In addition the really observed delay is not exactly 6 s, but can vary of ± 1 s from one mode to the other (value deduced from the Table 4). This possible 1 s error in the timing correction may give a false coincidence of 2 successive splitted modes after $\simeq 30$ h.

7. The intrinsic phase of p modes

For the second period of measurements (see Sect. 2), the observed phase Φ_g is calculated as in Sect. 3, but a narrower ± 3 μ Hz wide filter allows to separate the modes of degree $l = 0, l = 1$ and $l = 2$. Due to the 10 s hardware delay described in Sect. 2 we can calculate the real delay $\delta_{n,l}$ for a given mode of period $T_{n,l}$ and finally the real phase of the same mode:

$$\delta_{n,l} = \Phi_g / 2\pi \cdot T_{n,l} + 10$$

$$\Phi_{n,l} = \delta_{n,l} / T_{n,l}$$

The Table 4 gives the values of Φ_g , $\delta_{n,l}$ and the resulting delay for the phase $\Phi_{n,l}$. Fig. 6 shows $\Phi_{n,l}$ vs. the order n and the degree l of the p mode, with a clear decrease with l and a probable increase with n . The filters used for the p -mode selection may be a point of concern. At least, the major part of any mode goes through, and there are no sidelob in the spectrum to increase the natural cross-talk due to the statistical behaviour of the p modes.

Table 4. The delay corrected from the hardware lag and the intrinsic phase $\Phi_{n,l}$ deduced from the phase Φ_g of the p modes observed in the period 2 from Feb 18 to Mar 31, 1996, for the opposite of the signal in the red wing and the signal in the blue wing.

n,l	energy	Φ_g (d $^\circ$)	delay (s)	$\Phi_{n,l}$ (d $^\circ$)
17, 0	0.06	3.64	14.05	12.62
18, 0	0.09	4.27	14.51	13.74
19, 0	0.20	5.99	16.02	15.94
20, 0	0.27	5.67	15.44	16.11
21, 0	0.37	4.20	13.85	15.12
22, 0	0.21	6.82	15.98	18.23
23, 0	0.41	5.84	14.91	17.73
24, 0	0.14	6.46	15.22	18.84
25, 0	0.23	7.29	15.67	20.16
26, 0	0.07	3.98	12.98	17.34
27, 0	0.09	4.44	13.21	18.29
28, 0	0.05	2.90	12.02	17.24
<hr/>				
17, 1	0.10	4.35	14.72	13.56
18, 1	0.08	6.49	16.69	16.18
19, 1	0.29	3.49	13.43	13.67
20, 1	0.45	3.91	13.66	14.57
21, 1	0.86	4.34	13.89	15.49
22, 1	0.72	2.71	12.33	14.35
23, 1	0.43	4.72	13.90	16.85
24, 1	0.36	2.79	12.21	15.41
25, 1	0.16	5.04	13.84	18.14
26, 1	0.18	3.95	12.91	17.55
27, 1	0.07	4.68	13.33	18.77
28, 1	0.06	1.95	11.34	16.53
<hr/>				
17, 2	0.09	-1.15	8.78	8.28
18, 2	0.13	-1.22	8.77	8.69
19, 2	0.14	-0.88	9.16	9.53
20, 2	0.52	-1.60	8.53	9.29
21, 2	0.36	-2.70	7.63	8.68
22, 2	0.24	-0.76	9.36	11.11
23, 2	0.20	-1.76	8.57	10.59
24, 2	0.18	-3.80	7.04	9.04
25, 2	0.12	-3.17	7.62	10.16
26, 2	0.07	0.35	10.25	14.17

To test the stability of the result, we first use a narrower filter ($\pm 1 \mu\text{Hz}$, cf. Fig. 7). Secondly we analyse the relatively short period 1, for which the correction of the hardware delay is -10 s, with the $\pm 3 \mu\text{Hz}$ filter (cf. Fig. 8). The result for the period 2 are not affected by the change of the band pass. Comparing the period 1 to the period 2, the general behaviour remains similar, but the noise is larger for the shorter run. We can conclude that if the results still contain a part of noise, the general trends are reproducible.

The Fig. 6 shows a lag in d $^\circ$ sensitive to the degree l and likely to the radial order n . This suggests a change in the ratio $r = I_T / I_V$, as discussed in Sect. 4. This n dependence may be due to the combination of the acoustical filtering of p modes with the altitude, related to the radial order, with the geometric integration on the solar disk, for which we have to take into

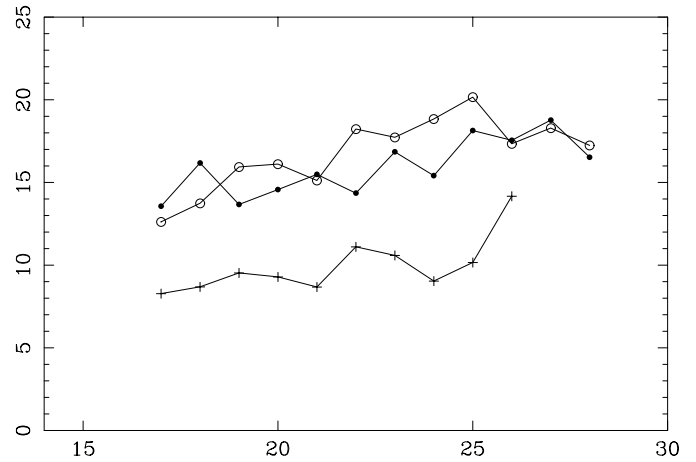


Fig. 6. The intrinsic blue-red phase delay for the period 2 vs. the order n for degree $l=0$ (\circ), $l=1$ (\bullet) and $l=2$ ($+$). The vertical scale is the phase in d $^\circ$. The horizontal scale is the radial order n .

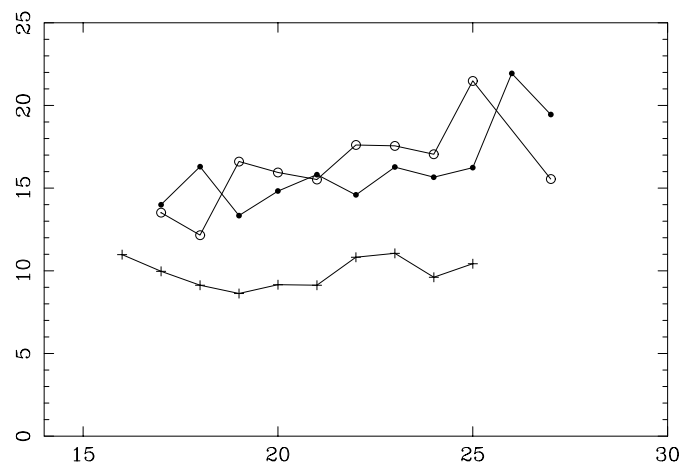


Fig. 7. The intrinsic blue-red phase delay for the period 2 vs. the order n for degree $l=0$ (\circ), $l=1$ (\bullet) and $l=2$ ($+$), but with a narrower filter than in Fig. 6. The vertical scale is the phase in d $^\circ$. The horizontal scale is the radial order n .

account the degree as well as the geometric altitude for the optical depth $\tau = 1$.

Further test of this result depends on availability of data. A come back to differential observation is not likely for GOLF, we have to turn to an analysis of the MDI observations (Scherrer et al., 1995), the ground-based observations analysis can also give a wide database. The MR5 experiment (Robillot et al., 1993) working on 2 optical depths in the DI sodium line is a good possibility of further progress. Nevertheless and before going farther, we have to solve the equations of the transfer of light in an atmosphere oscillating with p modes, together with the integration on the solar disk.

8. Simulation of the single p mode study

The results discussed in Sect. 7 are obviously uncertain, as they depend on a single experiment. As in Sect. 5 we use the observations of the period 3 to simulate a set of 18 experiments

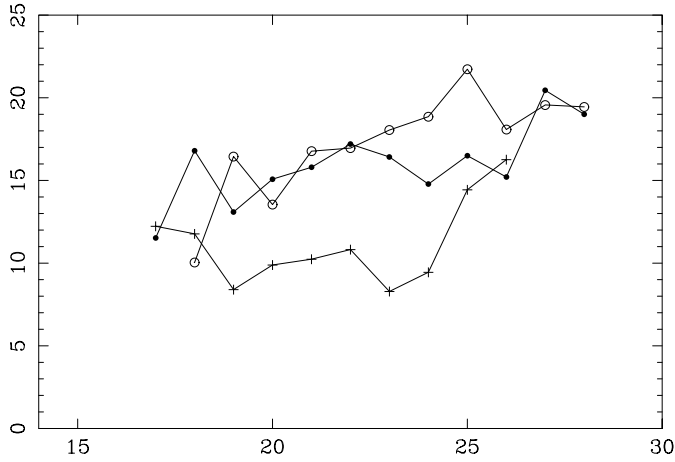


Fig. 8. The intrinsic blue-red phase delay for the period 1 vs. the order n for degree $l=0$ (\circ), $l=1$ (\bullet) and $l=2$ ($+$), with the large $3 \mu\text{Hz}$ filter. In spite of the lower statistical significance due to a shorter period of observation, the results for the high-energy modes are similar to Fig. 6. The vertical scale is the phase in $^\circ$. The horizontal scale is the radial order n .

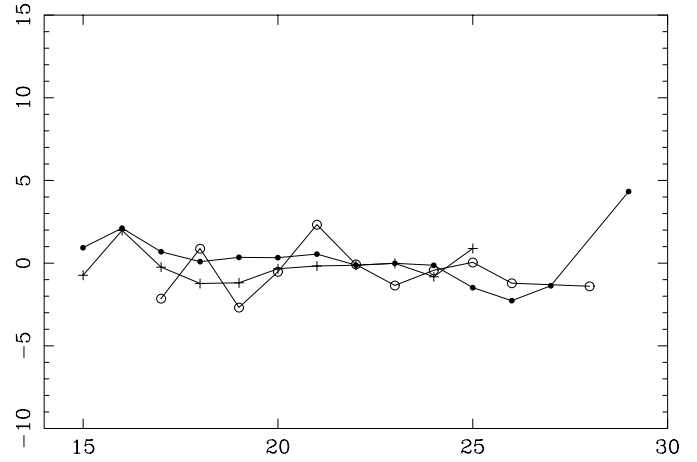


Fig. 9. The result of a simulated experiment using only the “blue” velocity measured period 3. The phase $\Phi_{n,l}$ is measured for the p mode of degree $l=0$ (\circ), $l=1$ (\bullet) and $l=2$ ($+$). The l, n effects visible in Fig. 6 are not visible. The vertical scale is the phase in $^\circ$. The horizontal scale is the radial order n .

equivalent to the period 2. We can evaluate the global uncertainty for a signal deduced from the blue wing observations. We show here the results after correction of the 10 s lag coming from the sequential nature of the measurements. The result for one simulated sequence is shown on the Fig. 9. The global result for the phase $\Phi_{n,l}$ and the standard deviation $\sigma_{n,l}$ are shown on the Fig. 10. The value of $\Phi_{n,l}$ is not dependent on l and probably not dependent on n . The standard deviation $\sigma_{n,l}$ is minimum for the high-energy modes. This result tends towards a confirmation of the solar origin of the results discussed in Sect. 7.

9. Conclusion

The present use of GOLF in a single wing mode gives only access to the “blue” velocity. This study confirms that for the p -mode velocity signal this “blue” velocity is $\simeq 6$ s in advance in respect of the “differential” velocity coming from other devices. This effect will make difficult any attempt to merge the GOLF data with data coming from a differential instrument to determine the p -mode splitting.

The relative delay of the red and blue signal should also be present in all differential devices. The daily drift of the working point along the solar line, changing the relative sensitivity to the velocity and the temperature components, may produce a small phase modulation for the p -mode signals.

The second point concerns the real properties of the solar “velocity” signal related to the p modes and is also relevant to all differential observations. The phase of intensity variations of the blue-shifted and red-shifted wings of the sodium lines are not purely in opposition and the difference observed, from 8° to 18° depends on the degree l and on the radial order n . If we believe this effect related to the temperature oscillations in the part of the photosphere where the D lines are produced, this effect produces an intensity modulation in the line wings more

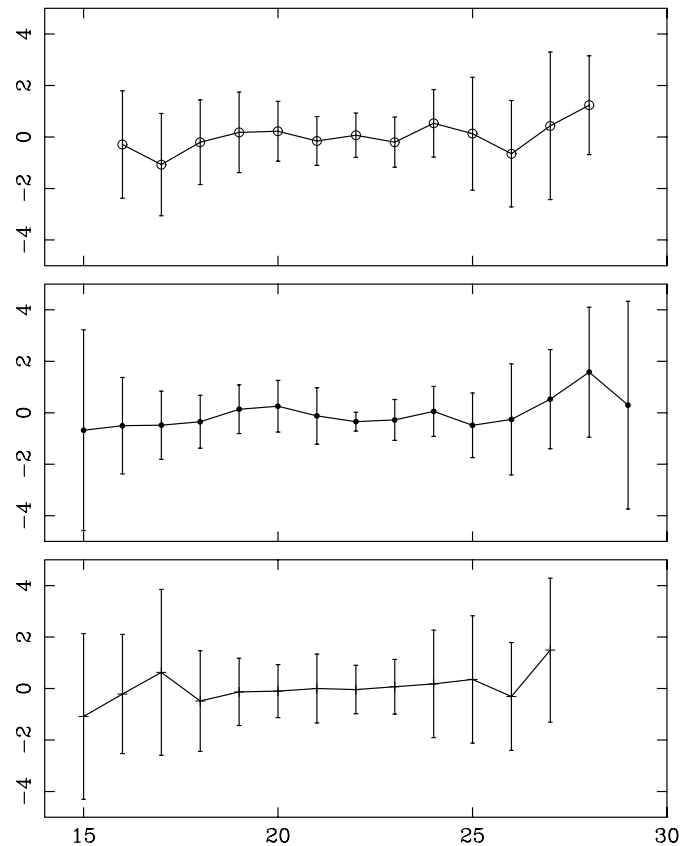


Fig. 10. The global result of the simulated observations using only the “blue” velocity. The phase $\Phi_{n,l}$ and the standard deviation $\sigma_{n,l}$ of the phase are measured for each p mode of degree $l=0$ (\circ , upper panel), $l=1$ (\bullet , central panel) and $l=2$ ($+$, lower panel). σ decreases as the energy of the modes increases. Neither l nor n dependence are observable. The vertical scale is the phase in $^\circ$. The horizontal scale is the radial order n .

than 4 to 5 times the modulation predictable from the white light signal. This result is sensitive to the degree l and likely sensitive to the radial order n . Pallé et al., 1999 analysing simultaneous data obtained from GOLF, MARK I (Brookes et al., 1978) and SOI-MDI (Scherrer et al., 1995) noticed a comparable delay for the “blue” GOLF velocity vs. the differential observations, and a comparable dependence to l .

The measure of the solar velocity is always deduced from the observation of a Fraunhofer line. Narrow fixed wavelength filters are used to measure the intensity in the wings, and the Doppler shift is deduced from the intensity changes. For this, the assumption of a fixed line profile is unavoidable when a differential instrument with 2 optical channels is used. We see there that firstly the profile of the D lines used by GOLF is partly linked to the temperature oscillations due to the p modes, secondly the line profile variations for a single p modes are n, l dependent, with measurable consequences for the study of p modes.

Acknowledgements. The GOLF instrument is due to a team issued from a consortium of institutes. The SOHO observatory is issued from a common project from ESA and NASA. The authors express their warm acknowledgments to their colleagues, scientists, engineers and technicians, for their dedication and motivation for the achievement of the good performances of the whole system.

References

- Brookes J.R., Isaak G.R., van der Raay H.B., 1978, Monthly Notices R.A.S. 185, p. 1
- Fröhlich C., Romero J., Roth H., et al., 1995, Solar Phys. 162, p. 101
- Gabriel A.H., Grec G., Charra J., et al., 1995, Solar Phys. 162, p. 61
- Henney C.J., Ulrich R.K., Bertello L., et al., 1998 In: Structure and dynamics of the interior of the sun and sun-like stars. SOHO 6 and GONG 98 workshop, Boston
- Jiménez A., Pallé P.L., Roca Cortés T. Domingo, V., 1988, A&A 193, p. 298
- Lazrek M., Baudin F., Bertello L., et al., 1997, Solar Phys. 175, p. 227–246
- Pallé P.L., Régulo C., Roca Cortés T., et al., 1999, A&A 341, p. 625
- Régulo, C., Roca Cortés T., Boumier P., et al., 1996, In: Provost J., Schmitter F.X. (eds.) Sounding solar and stellar interiors. Proceedings of Symposium IAU 181, Poster volume, OCA and UNSA, p. 55
- Robillot J.M., Bocchia R., Denis N., 1993, In: Large Scale Emergent Flows and Facular Region. Sixth IRIS workshop and GONG meeting, Cambridge, p. 37
- Scherrer P.H., Bogard R.S., Bush R.I., et al., 1995, Solar Phys. 162, p. 129
- Schrijver K., Jiménez A., Dappen W., 1991, A&A 251, p. 655
- Woodard M.A., Hudson H., 1983, Nat 305, p. 589